Computational Study of the C−H Bond Activation in Ethylene on a Binuclear Ruthenium Complex

Samat Tussupbayev and Sergei F. Vyboishchikov*

Institut de Química Computacional, Campus de Montilivi, Universitat de Girona, 17071 Girona, Catalonia, Spain

Received December 7, 2007

The reaction is substantially exothermic—the calculated total reaction enthalpy ΔH°_{298} between **1** + $6C_2H_4$ and **26** + $3C_2H_6$ is about −90 kcal·mol^{-1}. The reaction occurs through a number of stages, each including ethylene coordination, at least two hydride migrations, and ethane elimination. The rate-determining step of the mechanism is the initial coordination of the first ethylene molecule to the reactant **1** to give the ethylene π complex $(H)_2CpRu(\mu\text{-}H)_2RuCp(\eta^2\text{-}C_2H_4)$ (**2**). The free energy barrier is about 27 kcal·mol^{-1} according to the static DFT calculations. Metadynamic simulations of the coordination process yield a ΔG_{298} barrier of about 20 kcal·mol^{-1}. Another high-barrier step is the ethylene coordination to $CpRu(\eta^2{:}\eta^1\text{-}CH{=}CH_2)_2RuCp$ (**25**) to give the final product **26**. In total, the title reaction is a sophisticated multistep reaction with a large number of possible pathways. The mechanism of the reaction is largely determined by the flexibility of hydride ligands and by cooperation between both Ru centers.

Introduction

Polynuclear transition-metal complexes often exhibit unusual reactivity due to the cooperativity of multiple metal centers.[1] An important example is the diverse chemical activity of ruthenium polyhydride complexes with pentamethylcyclopentadienyl (Cp*) as auxiliary ligand toward a variety of substrates. Substantial experimental work in this area has been performed by Suzuki and co-workers.[2] A very versatile chemistry of such processes includes C−H bond activation,[3] C−C coupling, olefin insertion into a C−C bond,[4] Si−H bond activation,[5] and a number of other insertion reactions of the binuclear complex $Cp^*Ru(\mu\text{-}H)_4RuCp^*$.[6,7] On the other hand, the trinuclear complex $(Cp^*Ru)_3(\mu\text{-}H)_3(\mu_3\text{-}H)_2$ effects, for instance, alkane activation,[8] C=C bond cleavage in olefins,[9] N−N bond cleavage in hydrazine,[10] and N−H bond cleavage in ammonia.[11]

Characteristic of these complexes is a very high mobility of the hydride ligands. It influences their ability to coordinate an incoming ligand. A good example is the intermolecular hydrogen exchange reaction $(Cp^*Ru)_2(\mu\text{-}D)_4 + 2H_2 \rightarrow (Cp^*Ru)_2(\mu\text{-}H)_4 + 2D_2$.[3] In our previous computational work on the $(CpRu)_2(\mu\text{-}H)_4$ system (Cp = cyclopentadienyl)[12] we have shown that this reaction proceeds through various intermediate hexahydride complexes of the general formula $CpRu(H)_2(\mu\text{-}H)_2Ru(H)_2Cp$. It was also found that the hexahydride intermediates can easily transform into each other by means of the interconversion of the bridging and terminal hydrides, thus giving rise to additional exchange pathways.

Another process governing the chemistry of such complexes is the bridging ligand coordination to more than one metal center, with the manner of coordination changing during the course of the reaction. An example is the vinyl complex $Cp^*Ru(CH_2{=}CH_2)(CH{=}CH_2)_2RuCp^*$ containing Ru−C σ bonds to one ruthenium atom while coordinating in the η^2-π manner to the other.[4]

An interesting aspect of the reactivity of hydride ligands is demonstrated by the recent computational study of ethylene insertion into the Y−H bonds of the polyhydride complex $(\eta^5\text{-}C_5Me_4SiH_3)_4Y_4H_8$ with one μ_4-H, one μ_3-H, and six μ_2-H atoms.[13] It was found that the enthalpy barrier of the ethylene insertion into the Y−H bond of the triply bridged hydride is higher than that of the doubly bridged one. Both pathways lead to the same insertion product, where the resulting ethyl ligand adopts a μ_2-bridging structure.

The chemistry of the triruthenium complex $(Cp^*Ru)_3(\mu\text{-}H)_3(\mu_3\text{-}H)_2$ was studied experimentally in depth by Suzuki.[8–11] This complex exhibits reactivity toward a plethora of organic and inorganic substrates. Among others is the reaction of $(Cp^*Ru)_3(\mu\text{-}H)_3(\mu_3\text{-}H)_2$ with cyclopentadiene that leads to a C−C bond cleavage in the cyclopentadiene molecule. Originally, a dissociative mechanism via a $(Cp^*Ru)_3(\mu\text{-}H)_3$ intermediate was postulated. However, a thorough computational study by Khoroshun et al. revealed that the reaction proceeds through an associative mechanism with a large number of intermediates.[14] In this very sophisticated mechanism, many processes

* To whom correspondence should be addressed. Fax: +34 972 418356. Tel.: +34 972 418362. E-mail: vybo@stark.udg.edu.

(1) (a) Adams, R. A.; Cotton, F. A. *Catalysis by Di- and Polynuclear Metal Cluster Complexes*; Wiley-VCH: New York, 1998. (b) Doherty, S. *Organometallic Chemistry of Bi- and Poly-nuclear Complexes*; Royal Society of Chemistry: London, 1996; Annual Reports, Book A, pp 395−432.

(2) (a) Suzuki, H. *Eur. J. Inorg. Chem.* **2002**, 1009. (b) Takao, T.; Amako, M.; Suzuki, H. *Organometallics* **2003**, *22*, 3855. (c) Nakajima, Y.; Suzuki, H. *Organometallics* **2003**, *22*, 959. (d) Suzuki, H.; Kakigano, T.; Tada, K.; Igarashi, M.; Matsubara, K.; Inagaki, A.; Oshima, M.; Takao, T. *Bull. Chem. Soc. Jpn.* **2005**, *78*, 67. (e) Nakajima, Y.; Suzuki, H. *Organometallics* **2005**, *24*, 1860. (f) Shima, T.; Suzuki, H. *Organometallics* **2005**, *24*, 1703.

(3) Takao, T.; Suzuki, H.; Tanaka, M. *Organometallics* **1994**, *13*, 2554.

(4) Suzuki, H.; Omori, H.; Lee, D. H.; Yoshida, Y.; Fukushima, M.; Tanaka, M.; Moro-oka, Y. *Organometallics* **1994**, *13*, 1129.

(5) Tada, K.; Oishi, M.; Suzuki, H. *Organometallics* **1996**, *15*, 2422.

(6) Takao, T.; Yoshida, S.; Suzuki, H. *Organometallics* **2005**, *24*, 521.

(7) Inagaki, A.; Takemori, T.; Tanaka, M.; Suzuki, H. *Angew. Chem., Int. Ed.* **2000**, *39*, 404.

(8) Takemori, T.; Inagaki, A.; Suzuki, H. *J. Am. Chem. Soc.* **2001**, *123*, 1762.

(9) Nakajima, Y.; Suzuki, H. *Organometallics* **2003**, *22*, 959.

(10) Suzuki, H.; Kakigano, T.; Tada, K.; Igarashi, M.; Matsubara, K.; Inagaki, A.; Oshima, M.; Takao, T. *Bull. Chem. Soc. Jpn.* **2005**, *78*, 67.

(11) Nakajima, Y.; Kameo, H.; Suzuki, H. *Angew. Chem., Int. Ed.* **2006**, *45*, 950.

(12) Tussupbayev, S.; Vyboishchikov, S. F. *Organometallics* **2007**, *26*, 56.

(13) Luo, Y.; Hou, Z. *Organometallics* **2007**, *26*, 2941.

10.1021/om7012309 CCC: $40.75
Publication on Web 07/08/2008

Scheme 1. Mechanism of the C−H Bond Activation in Ethylene Proposed by Suzuki et al.[4]

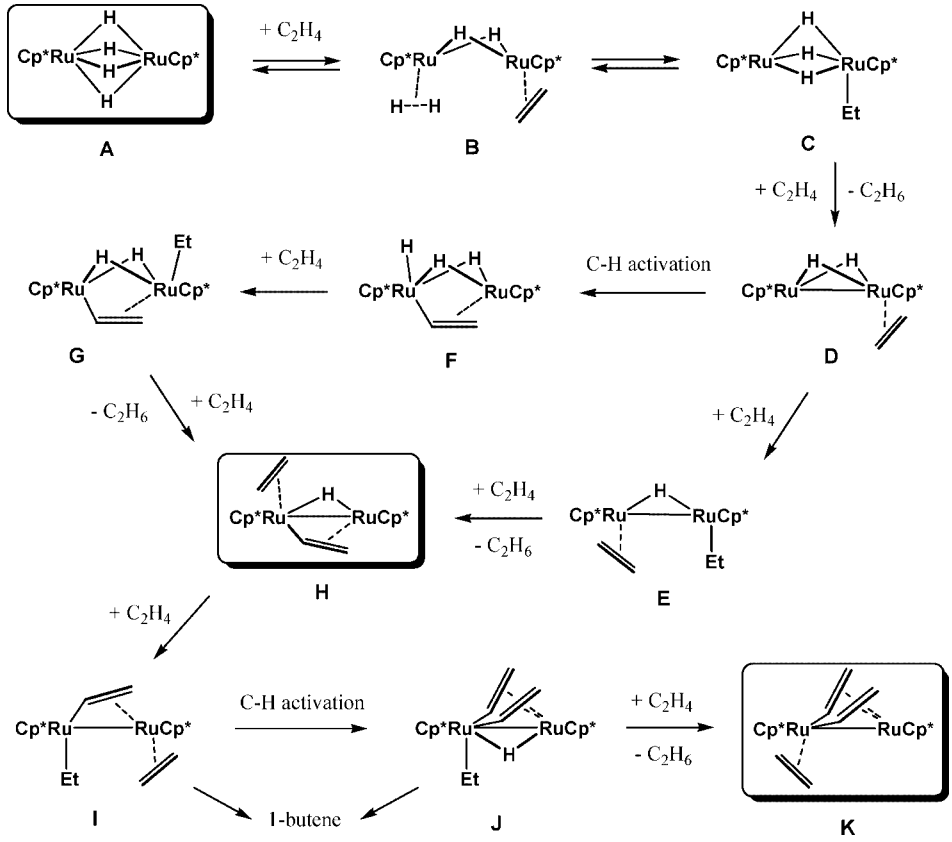

known in organometallic chemistry, such as oxidative addition, hydride−dihydrogen ligand isomerism, and agostic interactions interact to facilitate the reaction. Other computational studies regarding the reactivity of triruthenium complexes were published by Riehl et al.[15] and by Inagaki et al.[16]

Our current interest in binuclear complexes is aimed at determining how cooperating metals can influence the reactivity of catalytically relevant molecules, with a view toward modeling substrate activation by polynuclear clusters. The reactivity of the binuclear complex Cp*Ru(μ-H)$_4$RuCp* (**A**; eq 1) with respect to the intermolecular activation of the vinylic C−H bond of ethylene was studied experimentally by Takao et al.[3] The reaction of **A** with ethylene under atmospheric pressure at room temperature in toluene affords the bis(vinyl) complex Cp*Ru(C$_2$H$_4$)(μ-η^1:η^2-CHCH$_2$)$_2$-RuCp* (**K**). Complex **K** was shown to be formed through the intermediate mono(vinyl) complex Cp*Ru(C$_2$H$_4$)(μ-CH=CH$_2$)(μ-H)RuCp* (**H**). The latter was identified by the NMR technique but not isolated. It was suggested that it is highly reactive due to coordinative unsaturation at the metal centers and readily converts into **K** in the presence of excess ethylene.

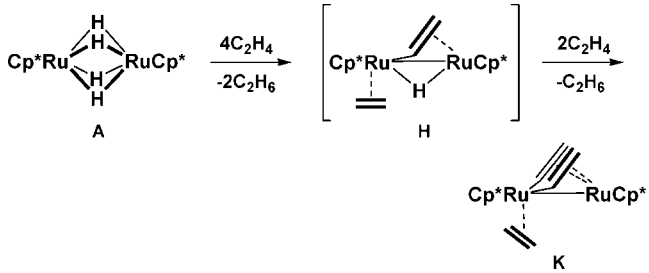

The C−H bond activation reaction can occur via either an associative or dissociative pathway: i.e., the first step of the reaction can be either the coordination of the first ethylene molecule or dihydrogen elimination. Koga and Morokuma's MP2//HF calculations[17] indicate that the dihydrogen dissociation from the model complex CpRu(μ-H)$_4$RuCp (**1**) to give coordinatively unsaturated CpRu(μ-H)$_2$RuCp is quite endothermic (ΔE_e = +57 kcal·mol^{-1}). In our recent study[12] of the intermolecular hydrogen exchange on **1**, we have shown at the DFT/BP86 level that this process is substantially less endothermic (ΔE_e = +37 kcal·mol^{-1}). However, the associative mechanism was still found to be much more favorable.

The associative mechanism shown in Scheme 1 was proposed on the basis of temperature-dependent ^{1}H NMR studies.[3] In this mechanism, the initial coordination and insertion of ethylene into a Ru−H bond yields the ethyl ruthenium species **C**. The latter reacts with a second ethylene molecule and undergoes reductive elimination of ethane to generate **D**. From here on, two pathways are possible, both leading to the intermediate **H** observed experimentally. The first route starts from the C−H bond activation to give the vinyl hydride complex **F**. It is followed by two ethylene coordination steps and the reductive elimination of ethane. In the alternative pathway, ethylene coordination precedes the cleavage of the vinylic C−H bond and occurs through intermediate **E**. Further coordination and insertion of ethylene into the Ru−H bond yield the ethyl vinyl complex **I**. The activation of the vinylic C−H bond in the latter leads to the ethylene bis(vinyl) complex **J**. Reductive elimination of ethane from **J** and the subsequent addition of ethylene finally afford the product complex **K**.

(14) Khoroshun, D. V.; Inagaki, A.; Suzuki, H.; Vyboishchikov, S. F.; Musaev, D. G.; Morokuma, K. *J. Am. Chem. Soc.* **2003**, *125*, 9910.
(15) Riehl, J.-F.; Koga, N.; Morokuma, K. *Organometallics* **1994**, *13*, 4765.
(16) Inagaki, A.; Musaev, D. G.; Toshifumi, T.; Suzuki, H.; Morokuma, K. *Organometallics* **2003**, *22*, 1718.
(17) Koga, N.; Morokuma, K. *J. Mol. Struct.* **1993**, *300*, 181.

Small amounts of l-butene were found, presumably as a result of a reductive coupling of the ethyl and vinyl ligands in **I** and/or **J**. We do not consider this process in the present paper.

In this work, we present a computational study of the mechanism of the C−H bond activation in ethylene on the complex $CpRu(\mu\text{-}H)_4RuCp$ to give the bis(vinyl) complex $CpRu(C_2H_4)(\mu\text{-}\eta^1{:}\eta^2\text{-}CHCH_2)_2RuCp$. It is obvious that, for reactions of such complexity, computational studies are an important complement to the experiment. Our main goal is to establish a detailed mechanism of the reaction, taking into account Suzuki's suggestion[3] (Scheme 1), by locating possible intermediates and the transition states. In order to get a deeper insight into the mechanism, we additionally performed metadynamics simulations of the rate-determining step of the reaction.

Computational Details

Static DFT Calculations. The computational study was performed with the complex $CpRu(\mu\text{-}H)_4RuCp$ (**1**). The replacement of Cp* by the cyclopentadienyl ligand (Cp) should not critically affect the chemistry but allows for large savings of the computer time.

The quantum-chemical calculations were carried out using density functional theory (DFT)[18] with the Gaussian 03 program package.[19] The gradient-corrected BP86 functional was employed, which combines Becke's nonlocal exchange[20] and Perdew correlation[21] functionals. We used the quasi-relativistic effective core potential of LaJohn et al. with the associate triple-ζ valence basis set[22] for ruthenium, 6-311G(d,p)[23] for the hydride hydrogens, and 6-31G(d,p)[24] for the spectator Cp ligands. For transition-metal compounds, the chosen DFT approach (BP86 functional with moderately large basis sets) normally provides realistic geometries, relative energies, and vibrational frequencies.[18,25] Metal hydride complexes are no exception.[25] A recent comparative study has shown that BP86 adequately describes agostic interactions in niobium complexes, while the popular B3LYP functional does not.[26] A number of test calculations for the reactant $CpRu(\mu\text{-}H)_4RuCp$ show that the chosen level of theory is well suited to describe the system under study.[12] The reactant, transition state, and product geometries were fully optimized without constraints. The nature of located stationary points was confirmed by computation of harmonic force constants. The transition states were connected to the related minima by means of an energy minimization following a small geometry displacement along the reaction coordinate obtained from the vibrational frequency calculation.

Metadynamics Calculations. The metadynamics method allows for an efficient sampling of the potential energy surface along one or several chosen internal coordinates (referred to as collective variables, CV). The characteristic feature of metadynamics is the gradual buildup of a biasing potential constructed by a superposition of small Gaussian hills depending on the values of the CVs. The biasing potential effectively pushes the system away from the reactant and product wells, allowing for sampling important transition states. The free energy profile is obtained from the accumulated biasing potential to arbitrary accuracy using sufficiently small Gaussian hills.

It is important that the CVs clearly distinguish reactants and products, as they determine the area of potential energy surface to be sampled. In the present study we used the coordination number (CN) between Ru and two C atoms of the ethylene ligand defined as

$$\mathrm{CN} = \frac{1}{2}\left(\frac{1-(r_{\mathrm{Ru-C1}}/r_0)^8}{1-(r_{\mathrm{Ru-C1}}/r_0)^{10}} + \frac{1-(r_{\mathrm{Ru-C2}}/r_0)^8}{1-(r_{\mathrm{Ru-C2}}/r_0)^{10}}\right)$$

where $r_{\mathrm{Ru-C1}}$ and $r_{\mathrm{Ru-C2}}$ are the distances between one of the ruthenium atoms and two carbon atoms of the ethylene ligand, correspondingly. The cutoff distance r_0 was taken as 2.2 Å.

The DFT metadynamics simulations were performed using the Born−Oppenheimer scheme as implemented in the CP2K-Quickstep code.[27,28] Quickstep is an implementation of the Gaussian plane wave (GPW) method.[29] The electronic structure calculations were done at the DFT level using the Perdew−Burke−Ernzerhof exchange and correlation functionals (PBE-PBE).[30] In this hybrid method the Kohn−Sham molecular orbitals are described by a linear combination of Gaussian-type orbitals, whereas an auxiliary plane-wave basis set is employed in order to expand the electron density. The triple-ζ basis set[27,31] on Ru, C, and H and the double-ζ basis set on the spectator Cp ligand in conjunction with the Goedecker−Teter−Hutter pseudopotentials[32] was used. The polarization functions were added for all atoms except Ru. The auxiliary plane-wave basis set was defined by a cubic box of 17 × 17 × 17 Å^3 and by an energy cutoff of 300 Ry. The interaction between periodic images was canceled using an isolation technique.[33]

After a series of test calculations, a Gaussian hill height was set to 0.5 kcal·mol^{-1} and the Gaussian width to 0.04 in CV units. The metadynamics step, i.e. the time interval between hills, was chosen to be 20 fs. The equations of motion were integrated using a time step of 1 fs, with a total simulation time of 23 600 fs, resulting to 1183 hills. The temperature was held within 300 K ± 50 K by rescaling atomic velocities.

(18) (a) Parr, R. G.; Yang, W. *Density Functional Theory of Atoms and Molecules*; Oxford University Press: New York, 1989. (b) Koch, W.; Holthausen, M. C. *A Chemist's Guide to Density Functional Theory*; Wiley-VCH: Weinheim, Germany, 2000.

(19) Frisch, M. J.; Trucks, G. W.; Schlegel, H. B.; Scuseria, G. E.; Robb, M. A.; Cheeseman, J. R.; Montgomery, J. A.; Vreven, T., Jr.; Kudin, K. N.; Burant, J. C.; Millam, J. M.; Iyengar, S. S.; Tomasi, J.; Barone, V.; Mennucci, B.; Cossi, M.; Scalmani, G.; Rega, N.; Petersson, G. A.; Nakatsuji, H.; Hada, M.; Ehara, M.; Toyota, K.; Fukuda, R.; Hasegawa, J.; Ishida, M.; Nakajima, T.; Honda, Y.; Kitao, O.; Nakai, H.; Klene, M.; Li, X.; Knox, J. E.; Hratchian, H. P.; Cross, J. B.; Bakken, V.; Adamo, C.; Jaramillo, J.; Gomperts, R.; Stratmann, R. E.; Yazyev, O.; Austin, A. J.; Cammi, R.; Pomelli, C.; Ochterski, J. W.; Ayala, P. Y.; Morokuma, K.; Voth, G. A.; Salvador, P.; Dannenberg, J. J.; Zakrzewski, V. G.; Dapprich, S.; Daniels, A. D.; Strain, M. C.; Farkas, O.; Malick, D. K.; Rabuck, A. D.; Raghavachari, K.; Foresman, J. B.; Ortiz, J. V.; Cui, Q.; Baboul, A. G.; Clifford, S.; Cioslowski, J.; Stefanov, B. B.; Liu, G., Liashenko, A.; Piskorz, P.; Komaromi, I.; Martin, R. L.; Fox, D. J.; Keith, T.; Al-Laham, M. A.; Peng, C. Y.; Nanayakkara, A.; Challacombe, M.; Gill, P. M. W.; Johnson, B.; Chen, W.; Wong, M. W.; Gonzalez, C.; Pople, J. A. Gaussian 03, Revision C.02; Gaussian, Inc., Wallingford, CT, 2004.

(20) Becke, A. D. *Phys. Rev. A* **1988**, *38*, 3098.

(21) Perdew, J. P. *Phys. Rev. B* **1986**, *33*, 8822.

(22) LaJohn, L. A.; Christiansen, P. A.; Ross, R. B.; Atashroo, T.; Ermler, W. C. *J. Chem. Phys.* **1987**, *87*, 2812.

(23) Krishnan, R.; Binkley, J. S.; Seeger, R.; Pople, J. A. *J. Chem. Phys.* **1980**, *72*, 650.

(24) Hehre, W. J.; Ditchfield, R.; Pople, J. A. *J. Chem. Phys.* **1972**, *56*, 2257.

(25) (a) Ziegler, T. *Chem. Rev.* **1991**, *91*, 651. (b) Ziegler, T. *Can. J. Chem.* **1995**, *73*, 743. (c) Jonas, V.; Thiel, W. *J. Chem. Phys.* **1995**, *102*, 8474. (d) See special issue on computational transition-metal chemistry: *Chem. Rev.* **2000**, *100*, 351−818.

(26) Pantazis, D. A.; McGrady, J. E.; Maseras, F.; Etienne, M. *J. Chem. Theory Comput.* **2007**, *3*, 1329.

(27) The CP2K developers group, http://cp2k.berlios.de, 2004.

(28) VandeVondele, J.; Krack, M.; Mohamed, F.; Parrinello, M.; Chassaing, T.; Hutter, J. *Comput. Phys. Commun.* **2005**, *167*, 103.

(29) Lippert, G.; Hutter, J.; Parrinello, M. *Mol. Phys.* **1997**, *92*, 477.

(30) Perdew, J. P.; Burke, K.; Ernzerhof, M. *Phys. Rev. Lett.* **1996**, *77*, 3865.

(31) Krack, M.; Parrinello M. *High Performance Computing in Chemistry*; Grotendorst, J., Ed.; Research Centre Jülich: Jülich, Germany, 2004; NIC series, Vol. 25; pp 29−51.

(32) (a) Goedecker, S.; Teter, M.; Hutter, J. *Phys. Rev. B* **1996**, *54*, 1703. (b) Krack, M. *Theor. Chem. Acc.* **2005**, *114*, 145.

(33) Martyna, G. J.; Tuckerman, M. E. *J. Chem. Phys.* **1999**, *110*, 2810.

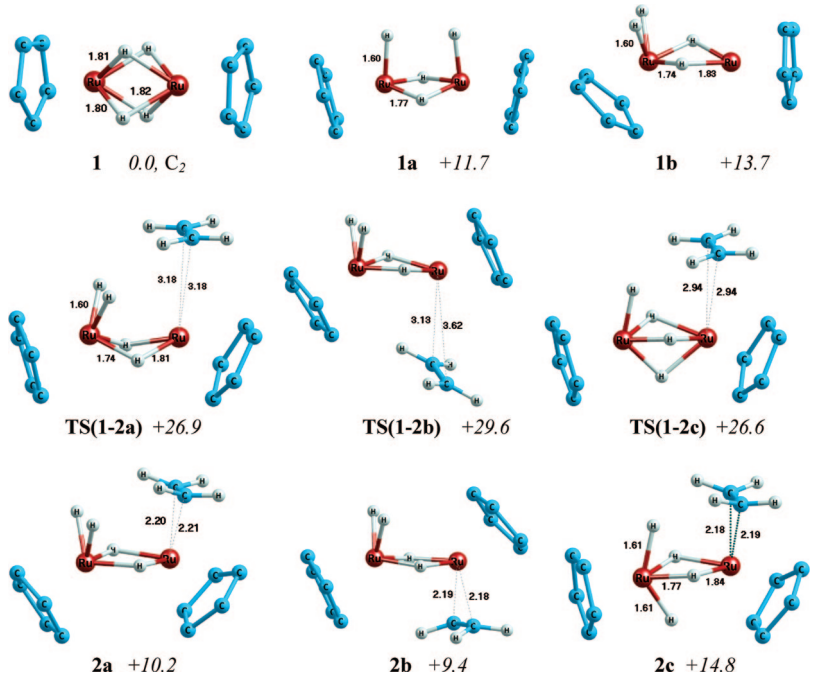

Figure 1. Optimized structures of the reactant **1**, its isomers **1a**,**b**, and transition states **TS(1-2a)**, **TS(1-2b)**, and **TS(1-2c)** corresponding to the first ethylene coordination process to give **2a**−**c**. The selected bond lengths are given in Å. The relative Gibbs free energies are given in kcal·mol^{-1}. Here and elsewhere in the paper the hydrogen atoms of the Cp rings are omitted for clarity.

Results and Discussion

We divided the whole mechanism depicted in Scheme 1 into four parts. Part 1 connects the reactant **A** and the intermediate **D**, parts 2 and 3 describe two alternative pathways of the consequent conversion of **D** into the experimentally observed intermediate **H**, and in part 4 the conversion of **H** into the final product **K** is considered.

A number of structures of the general formula $Cp_2Ru_2(H)_4$ found in our previous work[12] are shown in Figure 1. The 4-fold-bridged structure **1**, corresponding to the formula CpRu(μ-H)$_4$RuCp, was found to be a global minimum, in agreement with the experimental X-ray results.[3] The structure **1a** contains two terminal hydrides placed at each metal center in a cis orientation with respect to each other. In **1b**, both terminal hydrides are located on the same ruthenium atom, thus leaving the other ruthenium highly coordinatively unsaturated. **1a**,**b** are both extremely shallow and narrow minima, substantially less stable than **1** (ΔG°_{298} = +11.7 and +13.8 kcal·mol^{-1}, correspondingly).

Part 1 (A−D). According to the associative mechanism proposed by Suzuki (Scheme 1), the first step is the coordination of ethylene to complex **1**. The starting structures of the ethylene π complexes **2a**−**c** were obtained by attaching an ethylene molecule to **1** and **1b**. The most stable intermediates **2a**,**b** are π complexes with coordination energies ΔE_e = −4.4 and −4.4 kcal·mol^{-1} (Table 1); ΔG°_{298} = 10.2 and 9.4 kcal·mol^{-1}, correspondingly. **2c** is less stable (ΔE_e = 0.1 kcal·mol^{-1}; ΔG°_{298} = 14.8 kcal·mol^{-1}). The complexes **2a**−**c** are formed through the corresponding transition states **TS(1-2a), TS(1-2b)**, and **TS(1-2c)** with substantial $\Delta G^\ddagger_{298}$ barriers of +26.6, +29.6, and +26.9 kcal·mol^{-1}, correspondingly. Nevertheless, they are lower than the free energy barrier for the H_2 dissociation from **1** to give CpRu(μ-H)$_2$RuCp ($\Delta G^\ddagger_{298}$ = +34.2 kcal·mol^{-1}; see Scheme 2).[12] The optimized geometries of **TS(1-2a), TS(1-2b)**, and **TS(1-2c)** are shown in Figure 1. The barriers reflect high structure reorganization costs. The formation of the ethylene π complexes requires a rearrangement of the coordination sphere in **1** to generate a vacant site on one of the ruthenium atoms. Then, the incoming ethylene molecule is coordinated to the unsaturated ruthenium atom. The reverse step, i.e. ethylene elimination, would be accompanied by the simultaneous collapse of terminal hydrides. The $\Delta G^\ddagger_{298}$ barriers are also significant (+16.6, +20.2, and +11.7 kcal·mol^{-1}, respectively), indicating that **2a**−**c** are rather deep minima.

In principle, Scheme 2 suggests that there should be a direct pathway from the ethylene π complexes **2a**,**b** to **7**, merely as a result of reductive coupling of terminal hydrides and the subsequent dihydrogen elimination. It corresponds to the conversion of the intermediate **B** into **D** in the mechanism proposed by Suzuki (Scheme 1). The free energy barriers of dihydrogen elimination are 10.4 and 11.5 kcal·mol^{-1}, correspondingly. Thus, the calculations imply that direct H_2 dissociation should be preferred over the hydrogen uptake by the ethylene by 3−4 kcal·mol^{-1}. However, the experimental data indicate that direct H_2 elimination does not occur.[3]

The ethylene π complexes **2a**,**c** are likely to transform into each other in a way similar to that for the previously studied hexahydride complexes.[12] However, since the energy barriers of their formation from **1** are very close ($\Delta G^\ddagger_{298}$ = +26.6 and +26.9 kcal·mol^{-1}, respectively), their interconversion is not crucial for the mechanism under study.

According to the mechanism suggested by Suzuki et al.,[3] the following step is ethylene insertion into the Ru−H bond in the ethylene π complexes **2a**−**c**. The calculations show that the formation of ethyl complexes **4a**,**b** occurs through the β-agostic complexes **3a**−**c** (Scheme 2). The ethylene π complexes **2a**−**c** convert into the β-agostic complexes **3a**−**c** through the transition states **TS(2a-3a)**, **TS(2b-3b)**, and **TS(2c-3c)**, correspondingly. The free energy barriers of these transformations are +13.8, +14.4, and +11.8 kcal·mol^{-1}, respectively. The significant free energy barriers can be explained by the rupture of a strong bridging Ru−H−Ru bond in the four-center transition states **TS(2a-3a)** (Figure 2), **TS(2b-3b)**, and **TS(2c-3c)**. The newly forming C$^\beta$−H bond in the transition states is within 1.41−1.47

Table 1. Calculated Relative Equilibrium Energies (ΔE_e), Gibbs Free Energies (ΔG°_{298}) of Formation, and Entropy Contributions to Gibbs Free Energies ($-T\Delta S^\circ_{298}$) of the Reactant, Intermediates, and Products of Eq 1 in kcal·mol^{-1}

molecule	ΔE_e	ΔG°_{298}	$-T\Delta S^\circ_{298}$	molecule	ΔE_e	ΔG°_{298}	$-T\Delta S^\circ_{298}$
1 (A) + $6C_2H_4$	0	0	0	**TS(1-1a)** + $6C_2H_4$	10.9	11.8	−1.3
1a + $6C_2H_4$	10.7	11.7	−0.3	**1b** + $6C_2H_4$	13.7	13.7	0.4
			Part 1				
TS(1-2a) + $5C_2H_4$	14.1	26.9	10.4	**TS(3b-4b)** + $5C_2H_4$	14.2	29.0	11.3
TS(1-2b) + $5C_2H_4$	18.3	29.6	9.2	**TS(3c-4a)** + $5C_2H_4$	14.2	29.9	12.5
TS(1-2c) + $5C_2H_4$	14.1	26.6	11.0	**4a (C)** + $5C_2H_4$	−4.6	11.6	11.3
2a (B) + $5C_2H_4$	−4.4	10.2	11.7	**4b** + $5C_2H_4$	−9.0	7.6	11.8
2b + $5C_2H_4$	−4.4	9.4	11.2	**TS(4a-5)** + $5C_2H_4$	16.5	31.4	11.3
2c + $5C_2H_4$	0.1	14.8	11.8	**TS(4b-5)** + $5C_2H_4$	2.5	17.1	11.2
2d + $5C_2H_4$	21.2	35.2	11.7	**5** + $5C_2H_4$	−6.4	9.5	9.3
TS(2a-3a) + $5C_2H_4$	9.9	24.0	12.1	**6** + $5C_2H_4$ + C_2H_6	−2.9	2.7	−0.4
TS(2b-3b) + $5C_2H_4$	10.3	23.8	11.7	**TS(2a-7)** + $5C_2H_4$	8.5	22.4	10.9
TS(2c-3c) + $5C_2H_4$	12.7	26.6	12.0	**TS(2b-7)** + $5C_2H_4$	8.3	20.9	11.0
3a + $5C_2H_4$	9.2	24.9	11.9	**7 (D)** + $4C_2H_4$ + C_2H_6	−37.0	−17.0	12.1
3b + $5C_2H_4$	10.0	25.5	11.9	**TS(7-7′)** + $4C_2H_4$ + C_2H_6	−33.6	−13.7	13.0
3c + $5C_2H_4$	11.7	26.1	11.0	**7** + $4C_2H_4$ + C_2H_6	−38.2	−18.2	13.0
TS(3a-4a) + $5C_2H_4$	11.1	26.2	11.5				
			Part 2				
TS(7′-8) + $4C_2H_4$ + C_2H_6	−25.2	−7.8	13.2	***cis*-10a** + $3C_2H_4$ + C_2H_6	−37.5	−2.9	25.9
8 + $3C_2H_4$ + C_2H_6	−28.7	−10.9	12.7	***trans*-10a** + $3C_2H_4$ + C_2H_6	−36.7	−3.1	25.3
TS(8-cis-9a) + $3C_2H_4$ + C_2H_6	−24.0	3.9	21.0	**TS(*cis*-10a-*cis*-11a)** + $3C_2H_4$ + C_2H_6	−35.4	−1.8	24.8
TS(8-trans-9a) + $3C_2H_4$ + C_2H_6	−23.4	4.0	21.6	***cis*-11a (G)** + $3C_2H_4$ + C_2H_6	−37.5	−4.3	24.1
TS(8-*cis*-9b) + $3C_2H_4$ + C_2H_6	−21.9	8.1	24.8	**TS(cis-11a-cis-11a′)** + $3C_2H_4$ + C_2H_6	−36.6	−2.1	26.0
TS(8-*trans*-9b) + $3C_2H_4$ + C_2H_6	−18.8	11.0	23.8	***cis*-11a′** + $3C_2H_4$ + C_2H_6	−39.8	−6.0	24.8
***cis*-9a** + $3C_2H_4$ + C_2H_6	−49.6	−16.8	25.5	***trans*-11a** + $3C_2H_4$ + C_2H_6	−35.6	−1.5	25.0
***trans*-9a** + $3C_2H_4$ + C_2H_6	−51.5	−18.5	25.6	**TS(*cis*-11a′-12)** + $3C_2H_4$ + C_2H_6	−24.6	7.6	24.5
cis-9b + $3C_2H_4$ + C_2H_6	−49.5	−15.7	26.0	**12** + $3C_2H_4$ + $2C_2H_6$	−38.4	−16.8	12.2
trans-9b + $3C_2H_4$ + C_2H_6	−49.9	−18.0	25.0	**TS(12-13b)** + $2C_2H_4$ + $2C_2H_6$	−36.4	−5.7	20.8
TS(*cis*-9a-*cis*-10a) + $3C_2H_4$ + C_2H_6	−36.0	−2.8	26.4	**13a (H)** + $2C_2H_4$ + $2C_2H_6$	−73.9	−37.6	24.7
TS(trans-9a-trans-10a) + $3C_2H_4$ + C_2H_6	−35.8	−2.9	26.1	**13b** + $2C_2H_4$ + $2C_2H_6$	−67.3	−30.5	25.4
			Part 3				
TS(7-cis-14) + $3C_2H_4$ + C_2H_6	−29.0	1.3	22.1	**cis-16** + $3C_2H_4$ + C_2H_6	−45.4	−10.7	24.4
TS(7-trans-14) + $3C_2H_4$ + C_2H_6	−30.4	−0.6	21.6	**trans-16** + $3C_2H_4$ + C_2H_6	−40.8	−6.1	23.8
cis-14 + $3C_2H_4$ + C_2H_6	−52.1	−16.9	26.0	**TS(cis-16-18)** + $3C_2H_4$ + C_2H_6	−38.7	−6.6	24.2
trans-14 + $3C_2H_4$ + C_2H_6	−53.3	−19.1	25.3	**TS(trans-16-17)** + $3C_2H_4$ + C_2H_6	−24.7	7.8	22.4
TS(cis-14-cis-15) + $3C_2H_4$ + C_2H_6	−35.8	−2.6	−27.7	**17** + $3C_2H_4$ + C_2H_6	−32.1	1.8	21.5
cis-15 + $3C_2H_4$ + C_2H_6	−36.0	−1.4	24.9	**18** + $3C_2H_4$ + C_2H_6	−39.1	−6.9	24.2
trans-15 + $3C_2H_4$ + C_2H_6	−36.2	−2.0	24.4	**TS(18-19)** + $3C_2H_4$ + C_2H_6	−33.8	−2.3	23.4
TS(cis-15-cis-16) + $3C_2H_4$ + C_2H_6	−35.4	−1.8	24.8	**19** + $3C_2H_4$ + C_2H_6	−41.6	−9.4	22.0
TS(trans-15-trans-16) + $3C_2H_4$ + C_2H_6	−38.8	−4.1	24.4				
			Part 4				
TS(13a-20) + C_2H_4 + $2C_2H_6$	−70.6	−23.4	35.1	**TS(22a-23a)** + C_2H_4 + $2C_2H_6$	−75.4	−23.7	39.0
TS(13b-20) + C_2H_4 + $2C_2H_6$	−65.1	−18.7	34.4	**23a** + C_2H_4 + $2C_2H_6$	−75.5	−23.5	38.4
20 + C_2H_4 + $2C_2H_6$	−96.7	−43.8	39.4	**TS(23a-24a)** + C_2H_4 + $2C_2H_6$	−72.8	−22.0	38.3
TS(20-21a) + C_2H_4 + $2C_2H_6$	−87.4	−35.6	39.1	**24a** + C_2H_4 + $2C_2H_6$	−84.2	−33.7	35.9
TS(20-21b) + C_2H_4 + $2C_2H_6$	−79.9	−29.1	38.3	**24b** + C_2H_4 + $2C_2H_6$	−81.9	−39.7	27.6
21a + C_2H_4 + $2C_2H_6$	−87.6	−34.9	38.6	**25a** + C_2H_4 + $3C_2H_6$	−89.0	−50.8	25.9
21b + C_2H_4 + $2C_2H_6$	−82.9	−30.6	38.3	**25b** + C_2H_4 + $3C_2H_6$	−81.8	−42.8	25.6
TS(21a-22a) + C_2H_4 + $2C_2H_6$	−78.9	−25.1	39.1	**TS(25a-26a)** + $3C_2H_6$	−77.6	−28.6	34.9
TS(21b-22b) + C_2H_4 + $2C_2H_6$	−79.1	−26.7	38.4	**TS(25b-26b)** + $3C_2H_6$	−79.4	−28.9	36.9
22a + C_2H_4 + $2C_2H_6$	−82.4	−28.7	38.4	**26a (K)** + $3C_2H_6$	−109.5	−53.9	39.7
22b + C_2H_4 + $2C_2H_6$	−80.9	−28.2	38.1	**26b** + $3C_2H_6$	−102.8	−47.3	39.6
TS(22b-24b) + C_2H_4 + $2C_2H_6$	−67.1	−16.3	38.6				

Å. It is still substantially elongated in the minima **3a**−**c** (1.23−1.25 Å), indicating a very strong β-agostic interaction. The minima **3a**−**c** are extremely shallow, with ΔE_e between them and the corresponding transition states **TS(2a-3a)**, **TS(2b-3b)**, and **TS(2c-3c)** below 1 kcal·mol^{-1}(Table 1). Moreover, the $\Delta G^{\ddagger}_{298}$ values of the reverse process for complexes **3a**,**b** are even slightly negative (−0.9 and −1.7 kcal·mol^{-1}, respectively). Thus, the potential energy surface in the interval between the minima **3a**−**c** and the corresponding transition states is very flat. The distance C^{β}−H can vary relatively freely within 1.2−1.5 Å.

The loss of the agostic Ru···H−C interaction in **3a**−**c** results in the collapse of one of the terminal hydrides to form a new bridging Ru−H−Ru bond (Scheme 2, Figure 2). As a result, the agostic ethyl complexes **3a**,**b** convert into the corresponding nonagostic complexes **4a**,**b**, while **3c** yields **4b**. This rearrangement is quite exothermic (ΔH°_{298} = −12.6, −17.8, and −19.3 kcal·mol^{-1}, correspondingly), and the energy barriers for this process are very low ($\Delta G^{\ddagger}_{298}$ = 1.3, 3.6, and 2.8 kcal·mol^{-1}, correspondingly). **4a**,**b** are particularly stabilized by the formation of strong bridging Ru−H−Ru bonds.[17] This assumption is corroborated by considerably higher stability of **4b** with three bridging hydrides, compared to **4a** with two bridging hydrides (ΔH°_{298} = −4.6 kcal·mol^{-1}). The complexes **4a**,**b** are comparable in stability to the ethylene π complexes **2a**−**c**.

The intramolecular migration of a bridging hydride to ethyl ligand in **4a**,**b** yields the ethane σ complex **5** (Scheme 2). Optimized geometries of the transition states **TS(4a-5)** and **TS(4b-5)** are shown in Figure 3. An elongated C−H bond (1.13 Å) in the ethane ligand indicates a significant d(Ru)−σ*(C−H)

Scheme 2. Calculated Steps of the First Part of the C−H Bond Activation Reaction Mechanism[a]

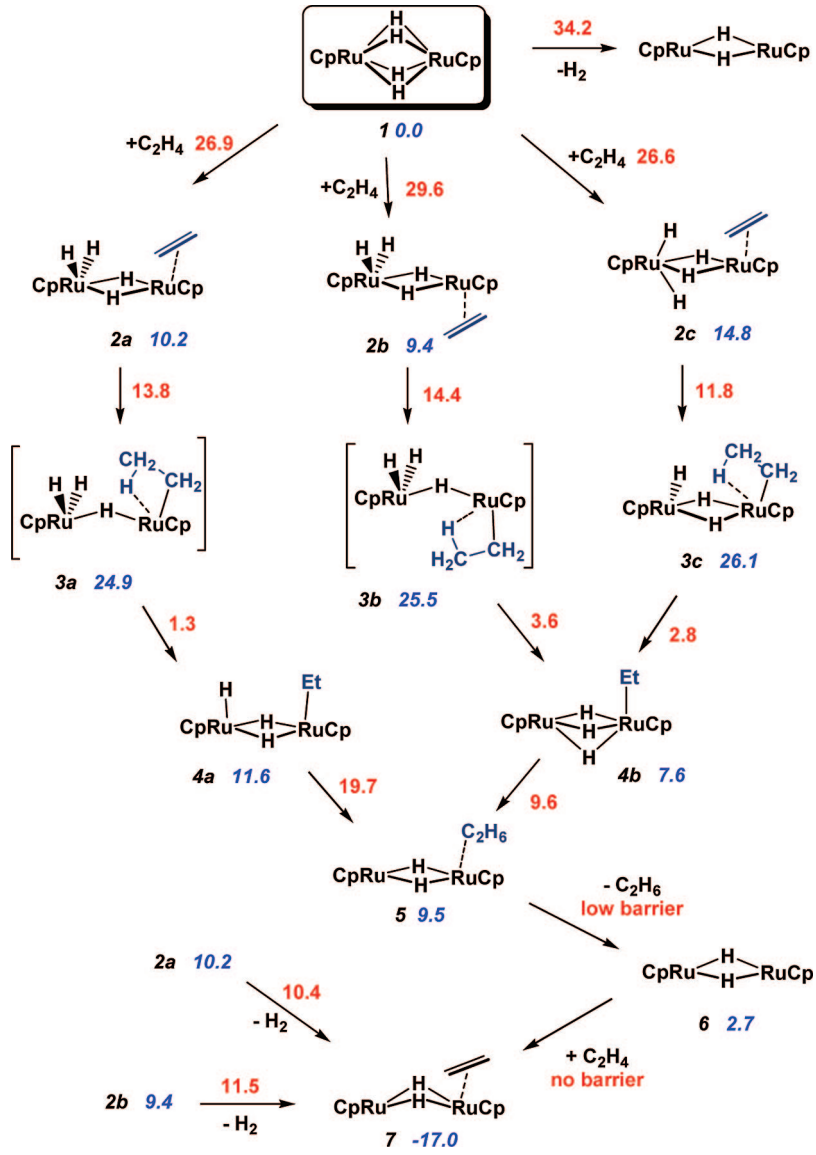

[a] Relative Gibbs free energies are given in kcal·mol^{-1}. The numbers above arrows are $\Delta G^{\ddagger}_{298}$ values in kcal·mol^{-1}.

back-donation in **5**. The migration of hydride in **4a** proceeds through **TS(4a-5)** with a substantially higher barrier ($\Delta G^{\ddagger}_{298}$ = +19.7 kcal·mol^{-1}) compared to that for **TS(4b-5)** ($\Delta G^{\ddagger}_{298}$ = +9.6 kcal·mol^{-1}). The reason **TS(4b-5)** is much more stable than **TS(4a-5)** (ΔE_e = −14.0 kcal·mol^{-1}) is the higher number of bridging hydrides in **TS(4b-5)**. A large difference in their energies confirms the strong stabilizing role of bridging hydrides.[17]

The reductive elimination of ethane from **5** in the gas phase is an effectively irreversible process, since ethane is free to leave into the gas phase. The elimination of ethane yields the highly unsaturated dihydride complex CpRu(μ-H)$_2$RuCp (**6**) (Scheme 2). It is a favorable process due to entropy effects (ΔH°_{298} = +2.9 kcal·mol^{-1}, ΔG°_{298} = −8.0 kcal·mol^{-1}). An optimization of the associate with the second ethylene added leads to the elimination of ethane, which indicates that the association from an energetic viewpoint facilitates the elimination of ethane. However, the associative step should be disfavored by entropy effects.

The coordination of the second ethylene molecule to **6** to give **7** is a highly exothermic process (ΔE_e = −34.1 kcal·mol^{-1}, ΔG°_{298} = −19.7 kcal·mol^{-1}). To check for a possible transition state, we performed a series of constrained-geometry optimizations with a fixed Ru−C distance at progressively longer distances. A monotonically increasing potential energy profile was obtained, which indicates that the process occurs without a barrier.

Since in **7** one of the Ru atoms is unsaturated (Figure 3), the existence of structures with ethylene coordinated to both Ru atoms was examined. This led to the minimum **7′** shown in Figure 3. Ethylene is asymmetrically bridging in **7′**, in an η^2 mode to one Ru and through an agostic Ru···H−C interaction to the other. The elongated C−H bond in the ethylene ligand (1.14 Å) in **7′** suggests a considerable d(Ru)−σ*(C−H) back-donation. This way of ethylene coordination provides **7′** an additional stabilization (ΔG°_{298} = −1.2 kcal·mol^{-1}) compared to **7**. The free energy barrier of the conversion of **7** to **7′** is 3.4 kcal·mol^{-1}. The geometry of **7′** suggests that this is an intermediate on the way of the transformation from the ethylene complex to the vinyl hydride species. Thus, the conversion of **7** to **7′** should facilitate the C−H bond activation in ethylene.

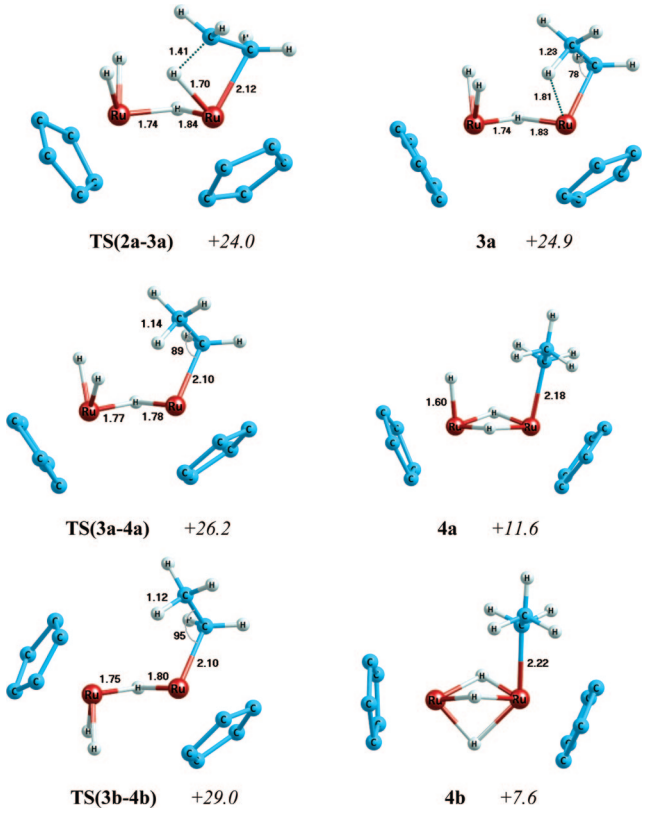

Figure 2. Optimized structures of the agostic ethyl complex **3a** and ethyl complexes **4a**,**b** and the transition states **TS(2a-3a)**, **TS(3a-4a)**, and **TS(3b-4b)** with selected bond lengths (in Å) and the relative Gibbs free energies (in kcal·mol^{-1}).

Part 2 (D−H). For the further stages of the reaction mechanism, two pathways are possible, as shown in Schemes 3 and 4. The first path starts from the intramolecular C−H bond activation in ethylene in **7′** to give the monovinyl complex **8** with a free energy barrier of +10.4 kcal·mol^{-1} (Scheme 3, Figure 3). The two Ru atoms in the resulting structure **8** are bridged by a μ-σ,π-vinyl ligand. The latter is 7 kcal·mol^{-1} less stable than the ethylene π complex **7** on the ΔG°_{298} scale.

The coordination of the third ethylene molecule to **8** can proceed in a number of ways. Depending on the metal center ethylene coordinates to and the orientation of ethylene with respect to two terminal hydrides (cis or trans), four resulting structures are possible: ***cis*-9a**, **trans-9a**, **cis-9b**, and **trans-9b** (Scheme 3). The free energy barriers of the formation of ***cis*-9a** and ***trans*-9a** are 4−7 kcal·mol^{-1} lower than those of **cis-9b** and **trans-9b** (Scheme 3). Therefore, from here on, only the more preferable **cis-9a** and **trans-9a** will be considered.

The ethylene coordination to **8** to yield **cis-9a** and **trans-9a** is a favorable process (ΔG°_{298} = −5.9 and −7.6 kcal·mol^{-1}, respectively). Substantial free energy barriers ($\Delta G^{\ddagger}_{298}$ = +14.8 and +14.9 kcal·mol^{-1}, respectively) are contributed to by entropy effects ($\Delta G^{\ddagger}_{298}$ = +6.5 and +6.3 kcal·mol^{-1}, respectively). Ethylene attack is accompanied by the rearrangement of hydrides in **cis-9a** and **trans-9a** (Scheme 3). One of the Ru−H−Ru bonds is broken to form a terminal hydride on one of the Ru atoms, thus generating a vacant place on the other.

The π complexes **cis-9a** and **trans-9a** undergo ethylene insertion into the Ru−H bond to yield the ethyl complexes **cis-11a** and **trans-11a** through the agostic complexes **cis-10a** and **trans-10a**, respectively (Scheme 3). This process is very similar to the conversion of **2a**−**c** into **4a**,**b** described above.

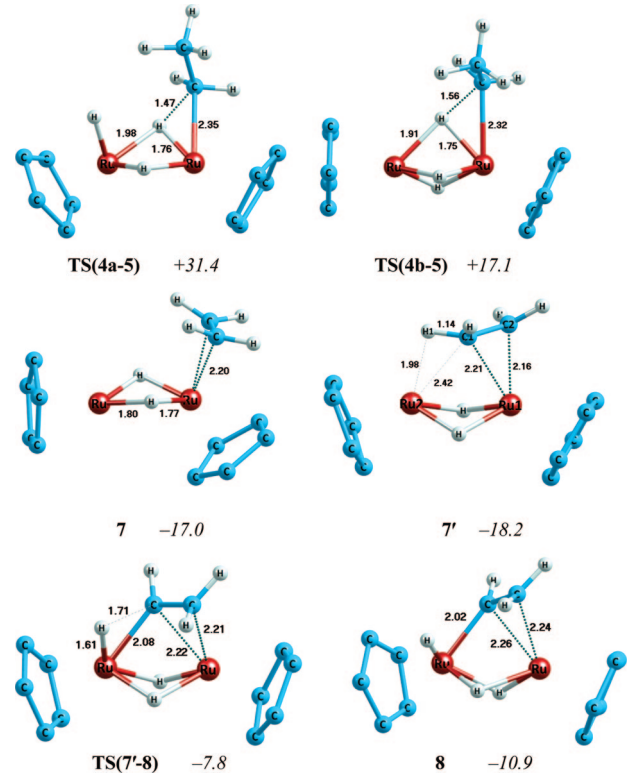

Figure 3. Optimized structures of the transition states **TS(4a-5)** and **TS(4b-5)** leading to the ethane σ complex **5** and of the η^2-coordinated ethylene π complex **7**, asymmetrically bridged ethylene π complex **7′**, the transition state of the C−H bond cleavage in ethylene **TS(7′-8)**, and the product vinyl hydride complex **8** with selected bond lengths (in Å) and the relative Gibbs free energies (in kcal·mol^{-1}).

The two terminal hydrides in **cis-11a** readily collapse to give the structure **cis-11a′** ($\Delta G^{\ddagger}_{298}$ = +2.2 kcal·mol^{-1}) (Figure 4). As a result of hydride rearrangement, one of them becomes bridging, while the other remains terminal, but in the trans position with respect to the ethyl ligand. The gain in energy is insignificant (ΔG°_{298} = −1.7 kcal·mol^{-1}). For **trans-11a** such a rearrangement of terminal hydrides is complicated sterically by the adjacent Cp ring.

The bridging hydride in **cis-11a′** further migrates to the ethyl ligand to directly produce the vinyl hydride complex **12** (Scheme 3, Figure 4). The migration proceeds through the transition state **TS(*cis*-11a′-12)** with a free energy barrier of +11.9 kcal·mol^{-1}. No minimum has been obtained for an ethane σ complex as the result of optimization, indicating that ethane leaves immediately.

Our calculations show that the coordination of the fourth ethylene molecule to **12** to yield **13a** (Scheme 3), which corresponds to the experimentally observed intermediate **H**, proceeds without a barrier. This is in line with a high exothermicity of the coordination process (ΔH°_{298} = −33.4 kcal·mol^{-1}, ΔG°_{298} = −20.8 kcal·mol^{-1}). We have also examined the possibility of ethylene coordination to the other ruthenium atom in **12** to yield **13b**. This way of coordination is less exothermic (ΔH°_{298} = −26.9 kcal·mol^{-1}, ΔG°_{298} = −13.7 kcal·mol^{-1}) and proceeds with a significant barrier ($\Delta G^{\ddagger}_{298}$ = +11.1 kcal·mol^{-1}).

Part 3 (D−H). Alternatively to the C−H bond activation in **7**, the coordination of the third ethylene molecule can occur. The incoming ethylene can attack in either the cis or trans position with respect to the coordinated ethylene ligand in **7** to

Scheme 3. Calculated Steps of the Second Part of the C−H Bond Activation Reaction Mechanism[a]

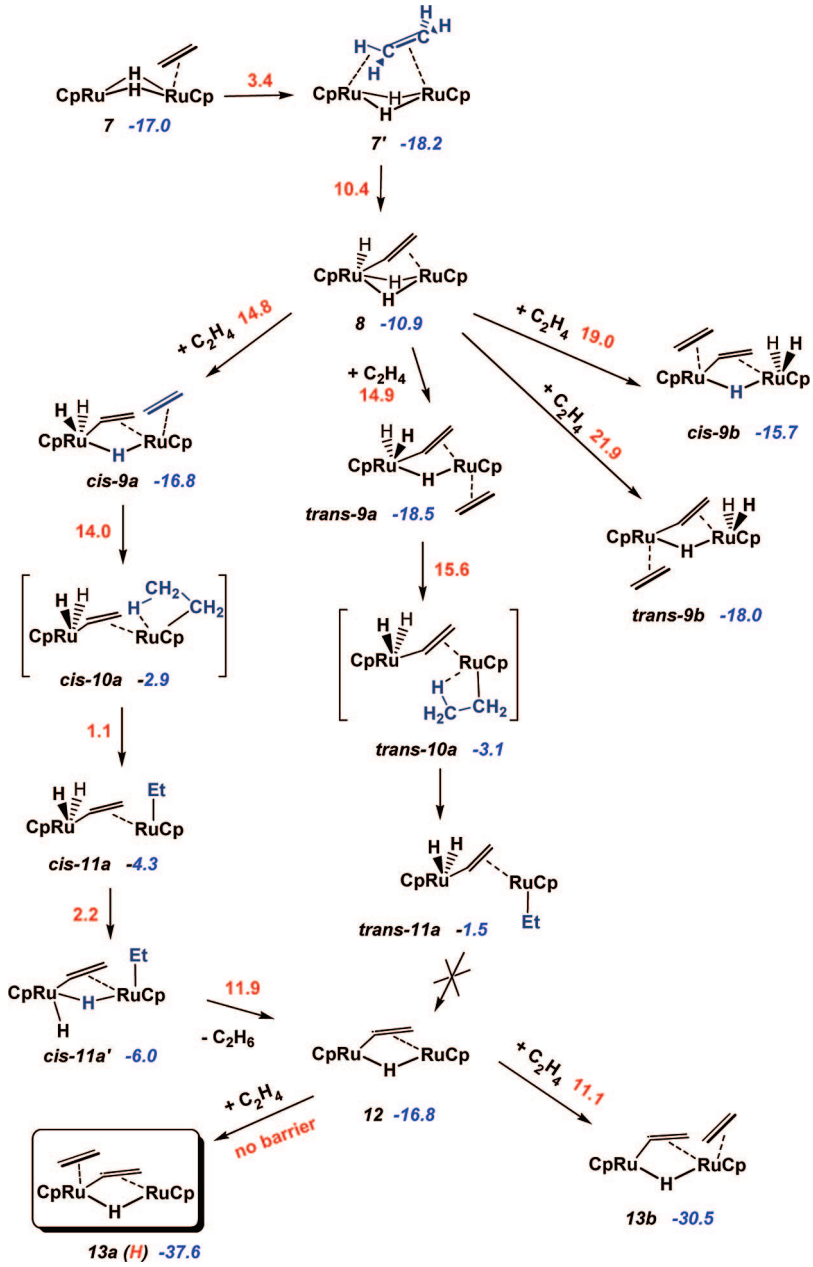

[a] Relative Gibbs free energies are given in kcal·mol^{-1}. The numbers above arrows are $\Delta G^{\ddagger}_{298}$ values in kcal·mol^{-1}.

yield the bis(ethylene) complexes **cis-14** and **trans-14** (Scheme 4). It is an exothermic process with ΔH°_{298} values of −13.8 and −15.3 kcal·mol^{-1}, respectively. The energy barriers of the coordination are significant (ΔH°_{298} = +8.3 and +6.9 kcal·mol^{-1}; $\Delta G^{\ddagger}_{298}$ = +18.3 and +16.4 kcal·mol^{-1}, respectively). These barriers reflect high energy costs associated with the tilt of a sterically demanding Cp ring.

The insertion of ethylene into the Ru−H bond in bis(ethylene) complexes **cis-14** and **trans-14** to yield ethyl complexes **cis-16** and **trans-16** occurs through the agostic complexes **cis-15** and **trans-15** (Scheme 4). The formation of **cis-15** and **trans-15** proceeds with significant energy barriers ($\Delta G^{\ddagger}_{298}$ = +15.5 and +17.1 kcal·mol^{-1}) through transition states **TS(*cis*-14-cis-15)** and **TS(*trans*-14-*trans*-15)**, correspondingly. Similarly to **3a−c**, **cis-15** and **trans-15** are very shallow and narrow minima. The conversion of **cis-15** and **trans-15** into respective **cis-16** and **trans-16** proceeds without a $\Delta G^{\ddagger}_{298}$ barrier, since the corresponding transition states **TS(*cis*-15-*cis*-16)** and **TS(*trans*-15-*trans*-16)** are lower than the corresponding minima (Table 1). **cis-16** is 4.6 kcal·mol^{-1} more stable than **trans-16** on the ΔG°_{298} scale. This is probably due to an additional stabilization of **cis-16** through asymmetrically coordinated ethylene ligand (Figure 5), as in **7′**.

The next step is the cleavage of the C−H bond in ethylene in ***cis*-16** to give vinyl-hydride complex **18**. The activation proceeds through the transition state **TS(*cis*-16-18)** (Figure 5). The free energy barrier of this process is $\Delta G^{\ddagger}_{298}$ = +4.1 kcal·mol^{-1}. Further the resulting terminal hydride migrates to the ethyl ligand in **18** to yield ethane σ complex **19** via transition state **TS(*cis*-18-19)** ($\Delta G^{\ddagger}_{298}$ = +4.6 kcal·mol^{-1}).

Part 4 (H−K). The final part of the mechanism (Scheme 5) starts from the coordination of the fifth ethylene molecule to **13a** or **13b** to produce the bis(ethylene) complex **20**. It is a favorable process (ΔG°_{298} = −6.2 and −13.3 kcal·mol^{-1},

Scheme 4. Calculated Steps of the Third Part of the C−H Bond Activation Reaction Mechanism[a]

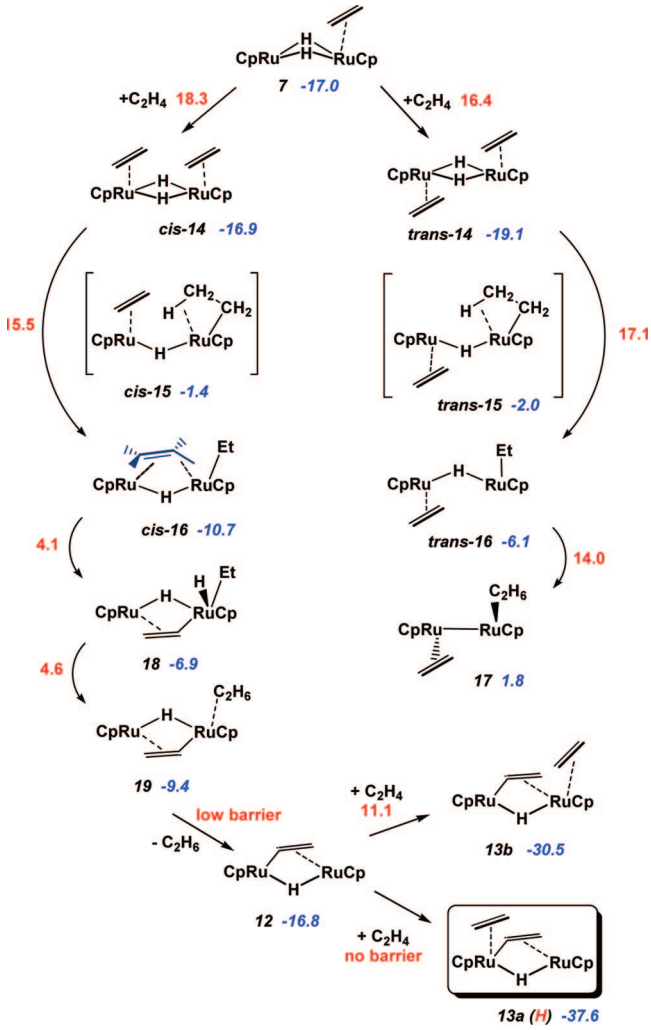

[a] Relative Gibbs free energies are given in kcal·mol^{-1}. The numbers above arrows are $\Delta G^{\ddagger}_{298}$ values in kcal·mol^{-1}.

respectively). The coordination proceeds with a lower barrier ($\Delta G^{\ddagger}_{298}$ = 11.8 kcal·mol^{-1}) for the less stable **13b** compared to **13a** ($\Delta G^{\ddagger}_{298}$ = 14.2 kcal·mol^{-1}).

Since either ethylene in **20** can be inserted into the corresponding hydride-bridged Ru−H−Ru bond, two subroutes, denoted **a** and **b**, are possible from here on (Scheme 5). Subroute **a** eventually leads to the product **26a**, corresponding to **K** in Scheme 1, while subroute **b** yields the alternative complex **26b**. The latter complex was not considered in Suzuki's original work.[3] The insertion of ethylene in both pathways to yield ethyl complexes **22a**,**b** occurs through agostic complexes **21a**,**b**, correspondingly. The insertion is an endothermic step (ΔH°_{298} = +16.0 and +16.9 kcal·mol^{-1}, respectively). Since **21a** is found to be a very shallow minimum, in pathway **a** the ethylene insertion should be considered as a one-step process leading directly from **20** to **22a** (Scheme 5). Consequently, the total energy barrier is considerable ($\Delta G^{\ddagger}_{298}$ = 18.7 kcal·mol^{-1}). The minimum **21b** is somewhat deeper than **21a**, and the formation of **22b** proceeds with lower barriers $\Delta G^{\ddagger}_{298}$ = 14.7 and 3.9 kcal·mol^{-1} through transition states **TS(20-21b)** and **TS(21b-22b)**, respectively.

Similarly to **7′**, ethylene ligand is asymmetrically bridged in **22a**,**b**, occupying a vacant space in the coordination sphere

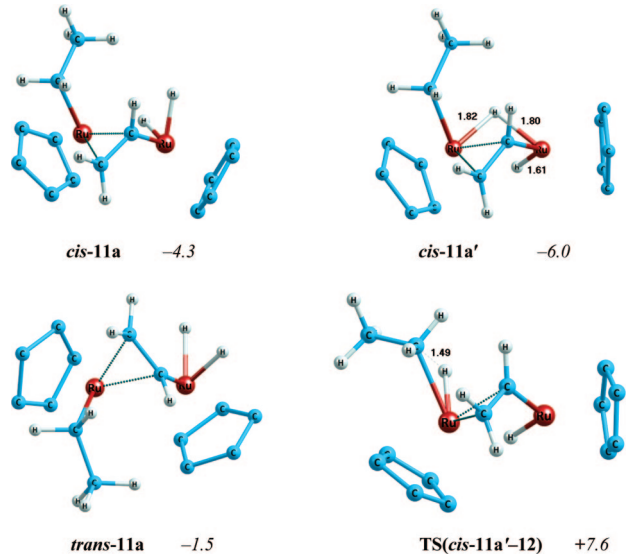

Figure 4. Optimized structures of ethyl complexes **cis-11a**, **cis-11a′**, and **trans-11a**, as well as of the corresponding transition state **TS(*cis*-11a′-12)**, leading to ethane elimination with selected bond lengths (in Å) and the relative Gibbs free energies (in kcal·mol^{-1}).

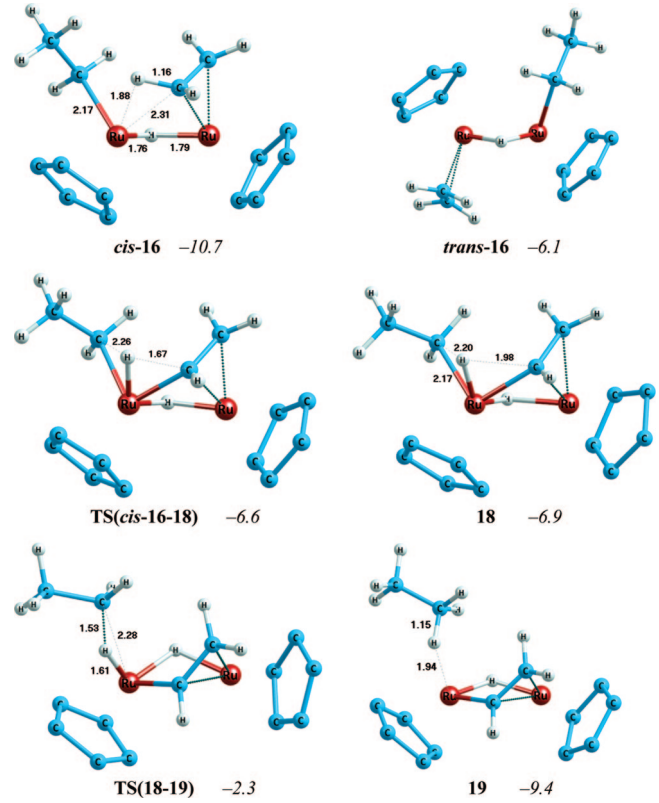

Figure 5. Optimized structures of nonagostic ethyl complexes **cis-16** with asymmetrically bridged ethylene and **trans-16** with η^2-coordinated ethylene and transition states **TS(*cis*-16-18)** and **TS(18-19)**, as well as corresponding product vinyl hydride ethyl **18** and ethane σ complex **19**. The selected bond lengths are given in Å and the relative Gibbs free energies in kcal·mol^{-1}.

released after the ethyl ligand loses an agostic interaction (Figure 6). Therefore, the C−H bond cleavage in **22a** to give the vinyl hydride complex **23a** proceeds with a low barrier ($\Delta G^{\ddagger}_{298}$ = 5.0 kcal·mol^{-1}). The minimum of **23a** is an extremely shallow one. It is only 0.1 kcal·mol^{-1} below the transition state **TS(22a-23a)** on the ΔE_e scale (Table 1). At the next stage, the hydride

Scheme 5. Calculated Steps of the Fifth Part of the C−H Bond Activation Reaction Mechanism[a]

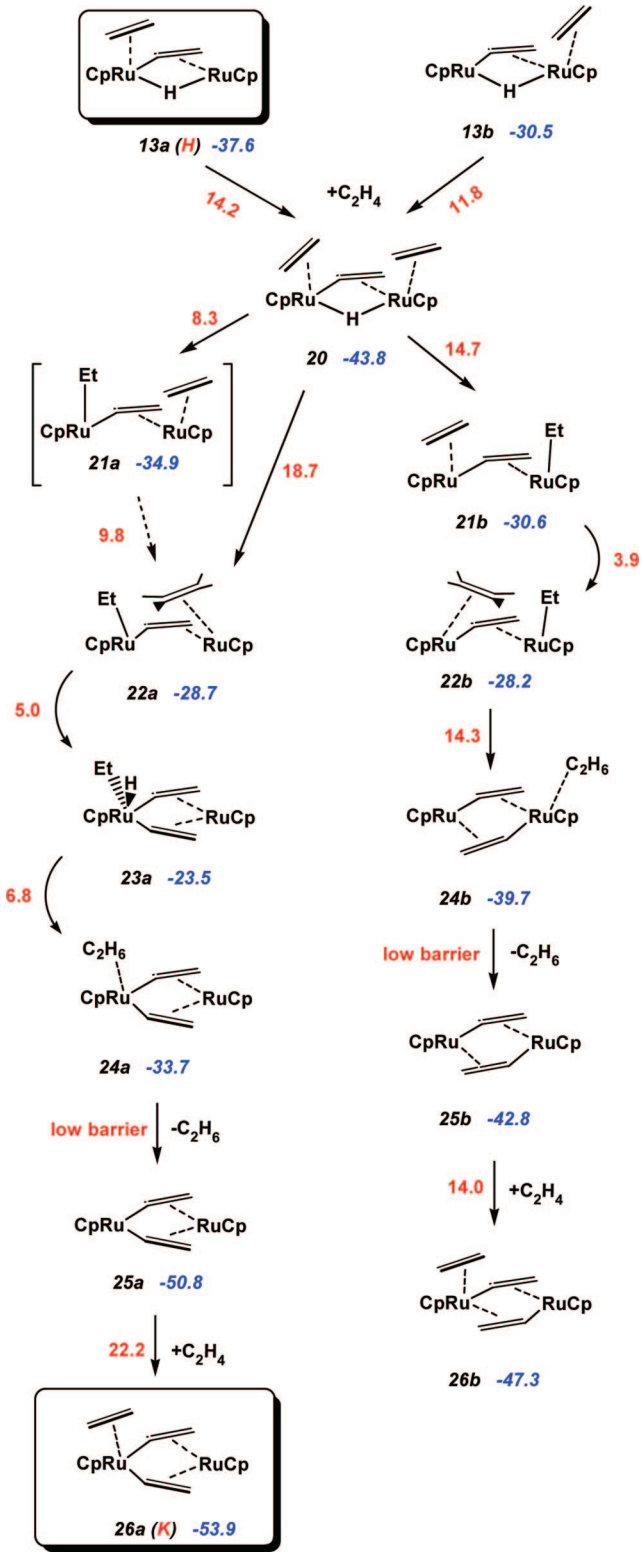

[a] Relative Gibbs free energies are given in kcal·mol^{-1}. The numbers above arrows are $\Delta G^{\ddagger}_{298}$ values in kcal·mol^{-1}.

ligand resulting from the cleavage migrates to the ethyl ligand to produce the ethane σ complex **24a** through the transition state **TS(23a-24a)** (Figure 7) with a $\Delta G^{\ddagger}_{298}$ barrier of 6.8 kcal·mol^{-1}. In **22b** both processes occur in a concerted manner through the transition state **TS(22b-24b)** (Figure 7). The energy minimization along the reaction coordinate for **TS(22b-24b)** leads to the

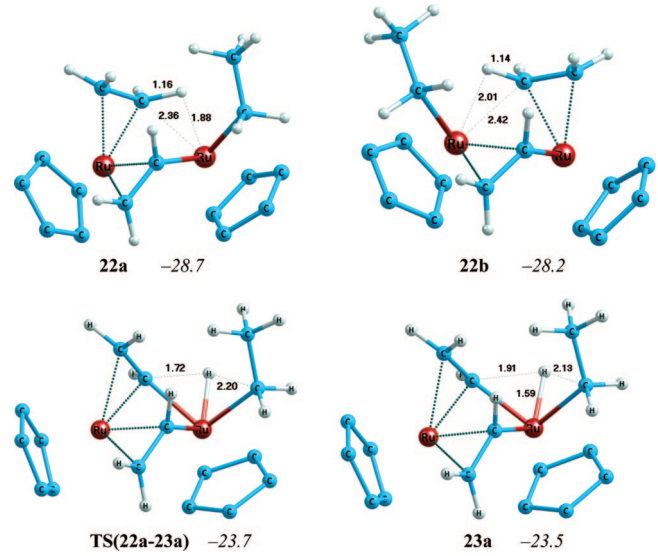

Figure 6. Optimized structures of nonagostic ethyl complexes **22a**,**b**, transition state **TS(22a-23a)**, and bis(vinyl) hydride complex **23a** with selected bond lengths (in Å) and the relative Gibbs free energies (in kcal·mol^{-1}).

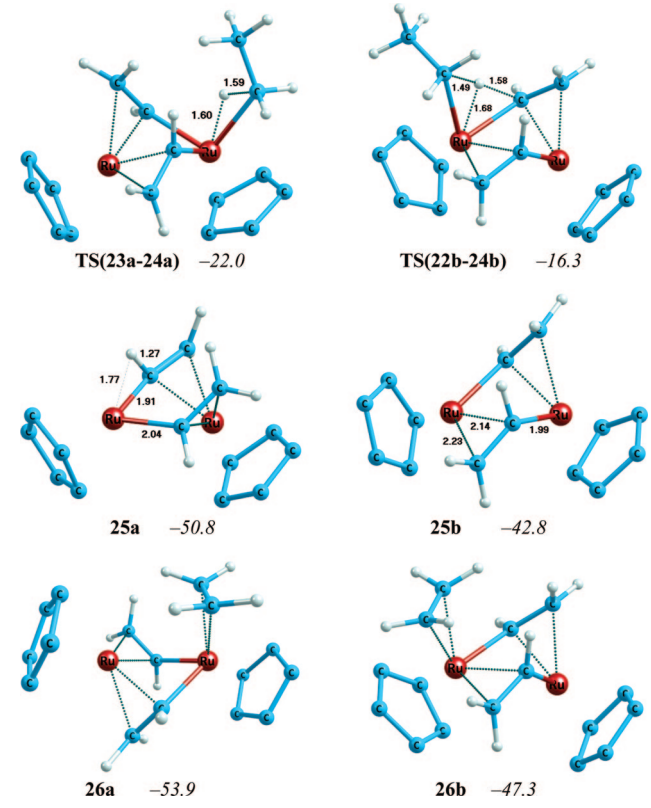

Figure 7. Optimized structures of transition states **TS(23a-24a)** and **TS(22b-24b)**, bis(vinyl) complexes **25a**,**b**, and final products **26a**,**b** with selected bond lengths (in Å) and the relative Gibbs free energies (in kcal·mol^{-1}).

ethane σ complex **24b** (Scheme 5). The $\Delta G^{\ddagger}_{298}$ barrier is 14.3 kcal·mol^{-1}, which is somewhat above the sum of the $\Delta G^{\ddagger}_{298}$ barriers of **22a** → **23a** and **23a** → **24a** (11.8 kcal·mol^{-1}).

The reductive elimination of ethane from **24a**,**b** yields bis(vinyl) complexes **25a**,**b**, respectively (Figure 7). Unexpectedly, the conversion **24a** → **25a** is an exothermic process (ΔH°_{298} = −7.1 kcal·mol^{-1}). It can be explained by the additional stabilization of **25a** due to an α-agostic interaction between the

ruthenium σ-bonded to both bridging vinyls and the C−H bond of one the vinyl ligands. As can be seen from Figure 7, the C^{α}−H bond in the corresponding vinyl ligand is strongly elongated (1.27 Å), while the Ru−C^{α} bond is rather short (1.91 Å).

The final step of the mechanism is the coordination of the sixth ethylene molecule to yield the bis(vinyl) ethylene complexes **26a** (**K** in Scheme 1) and **26b** (Scheme 5, Figure 7). The coordination is exothermic ($\Delta H^{\circ}_{298} = -16.9$ and -18.5 kcal·mol^{-1}, respectively). The coordination of ethylene to **25a** proceeds with a rather high energy barrier ($\Delta H^{\ddagger}_{298} = 13.3$ kcal·mol^{-1}, $\Delta G^{\ddagger}_{298} = 22.2$ kcal·mol^{-1}). It can be attributed to loss of the α-agostic interaction in **25a** in the course of the coordination (Figure 7). The energy barrier of the formation of **26b** is much lower ($\Delta H^{\ddagger}_{298} = 2.6$ kcal·mol^{-1}, $\Delta G^{\ddagger}_{298} = 14.0$ kcal·mol^{-1}, respectively). Thus, the pathway leading to the final product **26a** is in general harder to overcome than that leading to the species suggested by us, **26b**. However, the former is more preferred thermodynamically.

Metadynamics Results. As seen, the step of the mechanism with the highest barrier is the coordination of the first ethylene molecule to the reactant **1** to yield ethylene π complexes **2a**−**c**. The static DFT calculations yield a free energy barrier of about 27−29 kcal·mol^{-1} for this process. However, it should be borne in mind that the ethylene coordination is a bimolecular association process, in which the entropy has large contributions to the free energy. Moreover, the potential energy surface of hydride complexes is generally rather anharmonic.[34] The use of static methods can result in a significant error in estimation of entropy within the harmonic approximation. Molecular dynamics methods are more suitable to describe this type of reaction. Due to the height of the barrier, the use of metadynamics appears to be a natural choice. Therefore, a metadynamic study of the free energy surface of the process of ethylene coordination to **1** was performed. In so doing, we obtained a more pictorial description of the ethylene coordination and dissociation processes, which is reported in Figure 8 in the form of trajectory snapshots.

The starting point of the metadynamics simulation is the ethylene π complex **2a**. In the course of the ethylene dissociation process, both Ru−C distances increase almost symmetrically from the equilibrium value of 2.2 Å to about 2.6 Å (achieved at about 700 fs of the metadynamics simulation; Figure 8a). The π interactions still persist at such distances. At longer Ru−C distances, the ethylene elimination proceeds asymmetrically (Figure 8b). After about 2400 fs simulation time, the minimum well of **2a** is filled and the dissociation proceeds through a structure with three bridging hydrides (Figure 8c). It strongly resembles the geometry of the transition state **TS(1-2c)**. The dissociation of ethylene occurs simultaneously with the collapse of the terminal hydrides (Figure 8d). During the following 3000 fs, the minimum well of the dissociated **1** + C_2H_4 is filled. At about 5500 fs, the reverse process starts, and ethylene attacks the tetrahydride complex **1** to form **2a** through the transition state **TS(1-2a)**. After spending about 2000 fs around the minimum **2a**, the system passes to **2c**, which is higher in energy (Figure 8e). We described a similar transformation previously for hexahydride complexes with the general formula $Cp_2Ru_2H_6$.[12] During the following 2000 fs the system visits both minima **2a**,**c**, and at about 9600 fs of simulation time the dissociation of ethylene takes place. This time the elimination

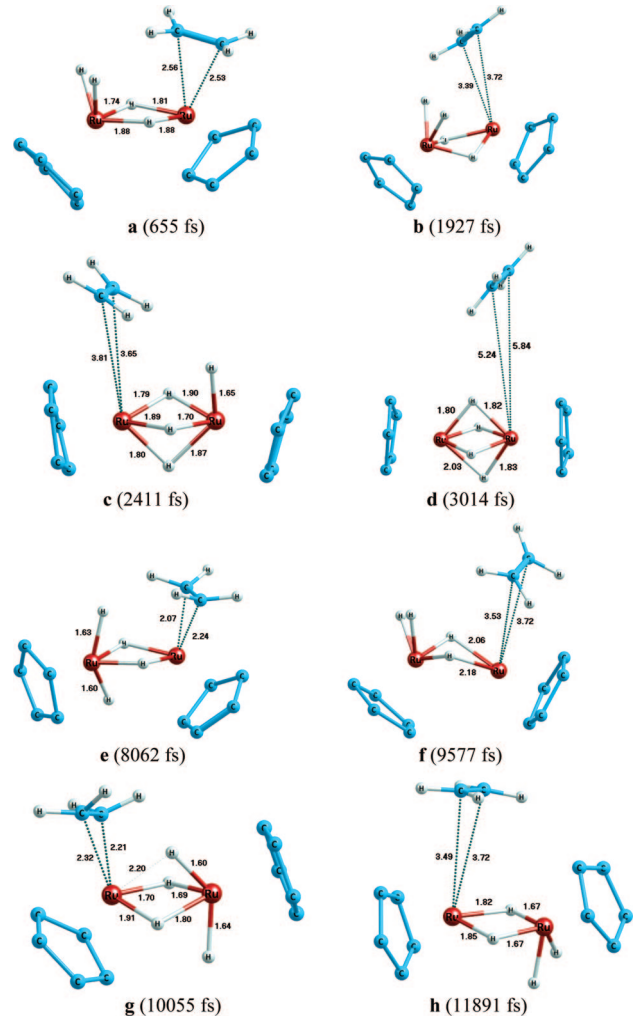

Figure 8. Snapshots from the metadynamics simulation of the ethylene elimination process **2a** → **1** + C_2H_4.

occurs through the structure depicted in Figure 8f. Then the system very rapidly returns to the initial **2a** and subsequently escapes to **2c**. At about 10 000 fs of simulation time, the system passes from **2c** to the more stable **2b** through the structure depicted in Figure 8g. The terminal hydride in **2c** substitutes the bridging one, while the formerly bridging one turns to terminal. At about 12 000 fs of simulation time, ethylene dissociates. This proceeds through a structure similar to **TS(1-2b)** (Figure 8h). From that point on, the oscillations of the collective variable become broad and the system freely visits all minima.

The metadynamics run gives a free energy profile (see Figure 9) as a function of the Ru−C_2H_4 coordination number (CN; see the exact definition in Computational Details). On this curve, all the species **2a**−**c** manifest themselves as a single minimum at a CN of about 1.4, while a deeper minimum at a CN of about 0.3 corresponds to the dissociated reactants. The metadynamics simulation yields an estimate of the Gibbs free energy difference ΔG°_{300} between **1** + C_2H_4 and **2a**−**c** of about −8 kcal·mol^{-1}. This compares reasonably with the static DFT value of −9.4 kcal·mol^{-1}. The activation free energy obtained from the metadynamics is about 20 kcal·mol^{-1}.

Conclusions

We have presented a scheme of the entire mechanism of the conversion of the binuclear ruthenium tetrahydride complex **1**

(34) (a) Maseras, F.; Lledós, A.; Clot, E.; Eisenstein, O. *Chem. Rev.* **2000**, *100*, 601. (b) McGrady, G. S.; Guilera, G. *Chem. Soc. Rev.* **2003**, *32*, 383.

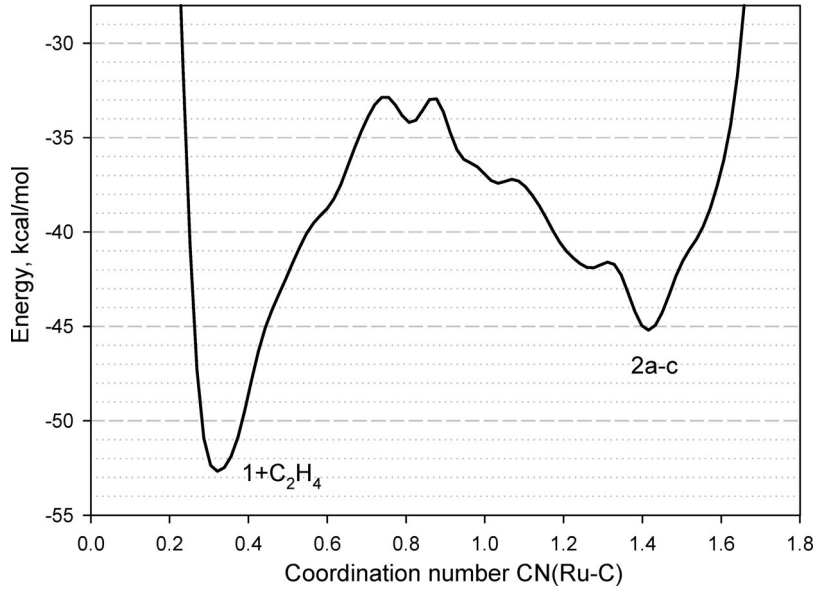

Figure 9. Free energy surface of the ethylene dissociation/coordination process from/to **2a**−**c** reconstructed by metadynamics at 300 K.

into the ethylene bis(vinyl) complex **26** in conjunction with ethylene hydrogenation. The reaction is substantially exothermic—the calculated standard enthalpy ΔH°_{298} between **1** (**A**) + $6C_2H_4$ and **26a** (**K**) + $3C_2H_6$ is about −90 kcal·mol^{-1}. The rate-determining step of the mechanism is the initial coordination of the first ethylene molecule to the reactant **1** to give the ethylene π complexes **2a**−**c**. The free energy barrier is about 27−29 kcal·mol^{-1} according to the static DFT calculations, while metadynamic calculations for the coordination process yield a $\Delta G^{\ddagger}_{300}$ barrier of about 20 kcal·mol^{-1}. Another high-barrier step is the ethylene coordination to **30a** to produce the final product **31a**. The corresponding free energy barrier is 22 kcal·mol^{-1} according to the static DFT calculations.

The results obtained indicate that the C−H bond activation of ethylene on dinuclear ruthenium species is a sophisticated multistep reaction with a large number of possible pathways. The mechanism of the reaction is largely determined by the flexibility of hydride ligands. The hydride ligands easily change from the bridging coordination to the terminal one. For instance, the initial ethylene coordination to **1** is accompanied by the conversion of two bridged hydrides into terminal ones. Further, in the course of the ethylene insertion into Ru−H bond they collapse, occupying a generated vacant space in **4**. This change between bridging and terminal coordination of hydrides is also inherent to the ethylene coordination to **8** and the following insertion step described in part 3 (Scheme 3). Essentially, the bridging hydrides play a role of an electron-mediating "buffer" facilitating the coordination of the incoming ethylene on the metal center and its further transformations.

The presented computational results altogether provide further support for the concept of cooperation between two Ru centers in a multistep transformation. The cooperative involvement of the two Ru centers in the C−H bond activation, as well as in the agostic interaction with the ethyl ligand at various stages of our mechanism is evident from Schemes 2–5. For instance, the C−H bond cleavage in ethylene π complex **7** occurs through the structure **7′** (Figure 3) with an asymmetric coordination of ethylene coordinated in the π manner to one Ru atom and through an agostic bond to the other.

Another example of the unusual reactivity of the binuclear complex attributed to the cooperativity of the metal centers is the C−H bond cleavage in ethylene in the complexes **22a**,**b**. The cleavage proceeds simultaneously with the migration of the resulting hydride to the ethyl ligand to form ethane.

The role of the hydride mobility can be best seen in the initial stages of the reaction (Scheme 2). First, a migration of the bridging hydride in **1** opens a vacant coordination site suitable to accept the incoming ethylene. Subsequently, the ethylene captures one of the remaining bridging hydrides to form an ethyl ligand. Simultaneously, a terminal hydride from the other ruthenium center turns to a bridging one, thus optimizing the coordination environment of the ruthenium. This bridging/terminal hydride interconversion is a major source of flexibility of the studied diruthenium hydride complexes, contributing essentially to the richness of their chemistry.

Acknowledgment. We are grateful to Prof. Jürg Hutter and Dr. Teodoro Laino (Universität Zürich) for stimulating discussions concerning the metadynamics method. Financial support from the Spanish Ministry of Education and Science (Ramón y Cajal Program and Grant No. CTQ2005-02698) is highly appreciated. S.T. thanks the Generalitat de Catalunya for a graduate fellowship.

Supporting Information Available: Tables giving Cartesian coordinates and absolute energies of all structures and figures giving molecular structures not shown in Figures 1–8. This material is available free of charge via the Internet at http://pubs.acs.org.

OM7012309